DOI: 10.1534/genetics.109.104208

Rrm3 Protects the *Saccharomyces cerevisiae* Genome From Instability at Nascent Sites of Retrotransposition

Radostina Stamenova, Patrick H. Maxwell, Alison E. Kenny and M. Joan Curcio[1]

Laboratory of Molecular Genetics, Wadsworth Center and Department of Biomedical Sciences, University at Albany School of Public Health, Albany, New York 12201-2002

Manuscript received April 20, 2009
Accepted for publication April 26, 2009

ABSTRACT

The DNA helicase Rrm3 promotes replication fork progression through >1000 discrete genomic regions and represses the cDNA-mediated mobility of the Ty1 retrotransposon. We explored the connection between DNA replication and Ty1 retromobility by investigating the basis of increased retromobility in an *rrm3* mutant. Even though Ty1 cDNA levels are increased in the absence of *RRM3*, neither the level nor target-site specificity of cDNA integration was altered. Instead, cDNA was incorporated into the genome by a Rad52-dependent mechanism that did not involve gene conversion of genomic Ty1 sequences. In *rrm3* isolates, incorporated cDNA was often present in tandem arrays. Multimeric cDNA arrays probably arise during chromosomal break repair, since their appearance was strongly correlated with the formation of gross chromosomal rearrangements. Moreover, Ty1 multimers were invariantly located on rearranged chromosomes, when present. Overexpression of a cellular RNase H, which degrades RNA in an RNA:DNA hybrid, completely suppressed the increase in Ty1 multimer formation in an *rrm3* mutant. We propose that RNA:DNA hybrid regions within nascent retrotransposition events block replication in an *rrm3* mutant, leading to chromosome breaks within Ty1 sequences. Multiple extragenomic Ty1 cDNA molecules are then used as donors in recombinational repair of the break before it is healed.

ALL of the mobile genetic elements in the nuclear genome of the yeast, *Saccharomyces cerevisiae*, are long terminal repeat (LTR) retrotransposons known as Ty elements. In their structure and replication cycle, Ty elements resemble infectious retroviruses, except that there is no extracellular phase in replication. The Ty RNA is encapsulated into cytoplasmic virus-like particles (VLPs), which consist of structural subunits encoded by *TYA* and three enzymatic proteins encoded by *TYB*: protease, integrase, and reverse transcriptase/RNase H. Inside the VLP, Ty RNA is reverse transcribed into a linear, double-stranded cDNA. The cDNA, in association with integrase, is transported back to the nucleus, where it is integrated into chromosomal DNA. While integration is the primary mode of Ty retromobility, Ty cDNA can also be incorporated into the genome by homologous recombination with genomic Ty elements (Melamed *et al.* 1992; Ke *et al.* 1999).

Ty1, present in ~30 copies per haploid genome, is the most abundant and most active of the retrotransposon families in budding yeast. The retromobility of Ty1 is repressed by a variety of proteins involved in genome stability. Ty1 repressors block cDNA synthesis, promote degradation of cDNA, or suppress cDNA recombination (Maxwell and Curcio 2007a). Examples of the latter class are Sgs1, a DNA helicase, and Rad27 (Fen1p), a FLAP endonuclease (Bryk *et al.* 2001; Sundararajan *et al.* 2003). In *sgs1*Δ and *rad27*Δ mutants, a large fraction of retromobility events are tandem arrays of Ty1 elements with a single LTR at the junction between elements. Multimeric Ty1 transposition events also occur at lower but easily detectable frequencies in wild-type strains. They are thought to form by recombination between Ty1 cDNAs prior to, during, or immediately after integration (Weinstock *et al.* 1990; Bryk *et al.* 2001). Multimeric Ty1 cDNA arrays can also be incorporated into the genome by homologous recombination with preexisting Ty1 sequences (Sharon *et al.* 1994; Maxwell and Curcio 2007b). Strikingly, Ty1 multimers that are inserted by homologous recombination are observed at chromosomal breakpoint junctions, raising the possibility that Ty1 cDNA arrays form in the process of chromosome break repair (Umezu *et al.* 2002; Maxwell and Curcio 2007b).

The *Saccharomyces cerevisiae* DNA helicases, Sgs1, Srs2, and Rrm3, are thought to have partially overlapping functions in maintaining genome stability during replication (Gangloff *et al.* 2000; Klein 2001; Fabre *et al.* 2002; Ooi *et al.* 2003; Schmidt and Kolodner 2004, 2006; Torres *et al.* 2004). These helicases are proposed to suppress inappropriate recombination intermediates

Supporting information is available online at http://www.genetics.org/cgi/content/full/genetics.109.104208/DC1.

[1]*Corresponding author:* Center for Medical Sciences, Wadsworth Center, P.O. Box 22002, Albany, NY 12201-2002. E-mail: curcio@wadsworth.org

TABLE 1

Strains used in this study

Strain	Genotype	Source
BY4741	*MAT***a** *his3Δ1 leu2Δ0 met15Δ0 ura3Δ0*	Open Biosystems
JC3884	*MAT***a** *his3Δ1 leu2Δ0 met15Δ0 ura3Δ0 rrm3Δ::kanMX*	Open Biosystems
JC3212	*MAT***a** *ura3Δ0 met15Δ0 leu2Δ0 his3Δ1* Ty1*his3AI-3114*	Mou *et al.* (2006)
JC3900	*MAT***a** *ura3Δ0 lys2Δ0 leu2Δ0 his3Δ1 rtt101Δ::kanMX* Ty1*his3AI-3114*	This study
JC3917	*MAT***a** *ura3Δ0 lys2Δ0 leu2Δ0 met15Δ0 his3Δ1 rrm3Δ::kanMX* Ty1*his3AI-3114*	Curcio *et al.* (2007)
JC3946	*MAT***a** *ura3Δ0 lys2Δ0 leu2Δ0 his3Δ1 rad51Δ::kanMX* Ty1*his3AI-3114*	This study
JC3956	*MAT***a** *ura3Δ0 lys2Δ0 leu2Δ0 his3Δ1 rad52Δ::kanMX* Ty1*his3AI-3114*	This study
JC4415	*MAT***a** *ura3Δ0 lys2Δ0 leu2Δ0 met15Δ0 his3Δ1 rrm3Δ::kanMX rad52Δ::hisG-URA3-hisG* Ty1*his3AI-3114*	This study
JC4522	*MAT***a** *his3Δ1 leu2Δ0 met15Δ0 ura3Δ0 URA3-tG(GCC)B*	This study
JC4526	*MAT***a** *his3Δ1 leu2Δ0 met15Δ0 ura3Δ0 rrm3Δ::kanMX URA3-tG(GCC)B*	This study
JC4733	*MAT***a** *his3Δ1 leu2Δ0 met15Δ0 ura3Δ0 ste12Δ::kanMX URA3-tG(GCC)B*	This study
JC4915	*MAT***a** *his3Δ1 leu2Δ0 met15Δ0 ura3Δ0 sgs1Δ::kanMX Ty1his3AI-3114*	This study
JC4916	*MAT***a** *his3Δ1 leu2Δ0 met15Δ0 ura3Δ0 srs2Δ::kanMX Ty1his3AI-3114*	This study
JC5266	*MAT***a** *ura3Δ0 lys2Δ0 leu2Δ0 met15Δ0 his3Δ1 rrm3Δ::kanMXΔNsi1 rad51Δ:KanMX* Ty1*his3AI-3114*	This study

that arise when replication forks stall or break. Sgs1 is a 3′- to 5′-DNA helicase in the RecQ family with a recently described role in resection of DNA ends at double-strand breaks (Gravel *et al.* 2008; Mimitou and Symington 2008; Zhu *et al.* 2008). The 3′- to 5′-DNA helicase Srs2 is an ortholog of UvrD that displaces the strand exchange protein Rad51 from single-stranded DNA (Krejci *et al.* 2003; Veaute *et al.* 2003). Rrm3 is a 5′–3′ helicase in the Pif1 family, which is conserved from yeast to humans. Rrm3 interacts with Orc5, PCNA, and Pol2 (epsilon), travels with the replication fork, and is involved in chromosomal DNA replication through nonnucleosomal protein:DNA complexes (Schmidt *et al.* 2002; Ivessa *et al.* 2003; Azvolinsky *et al.* 2006; Matsuda *et al.* 2007). In the absence of Rrm3, replication fork pausing and chromosomal breaks occur in the rDNA, telomeric and subtelomeric DNA, transcriptionally active tRNA genes, centromeres, inactive replication origins, the silent mating-type loci, and finally, in RNA polymerase II transcribed genes when the direction of transcription is opposed to the direction of replication (Ivessa *et al.* 2000, 2002, 2003; Prado and Aguilera 2005). Paradoxically, there is no increase in chromosome loss or gross chromosomal rearrangements in *rrm3* mutants (Ivessa *et al.* 2003; Schmidt and Kolodner 2006).

Rrm3 was identified as a repressor of the mobility of endogenous Ty1 elements in a genetic screen and was subsequently shown to repress Ty2 and Ty3 retromobility as well (Scholes *et al.* 2001; Irwin *et al.* 2005; Curcio *et al.* 2007). A marked increase in the level of unintegrated Ty1 cDNA accompanies the increased Ty1 retromobility in an *rrm3*Δ mutant, but surprisingly, integration of Ty1 into known hotspots is not elevated (Scholes *et al.* 2001; Curcio *et al.* 2007). In this work, we ask how this large pool of unintegrated Ty1 cDNA is incorporated into the genome in the *rrm3*Δ mutant. We show that deletion of *RRM3* increases the formation of tandem Ty1 cDNA arrays but does not increase integration or gene conversion of endogenous Ty1 elements. A high proportion of multimeric Ty1 arrays are present on rearranged chromosomes, supporting the idea that Ty1 multimers form during chromosome break repair. Given the ability of a related helicase, Pif1, to unwind RNA:DNA hybrids (Boule and Zakian 2007), we hypothesized that RNA:DNA hybrid regions in nascent Ty1 retrotransposition events block replication forks in the absence of Rrm3. Chromosome breaks ensue, and multimeric Ty1 cDNA arrays are incorporated into the genome during break repair. In support of this hypothesis, we show that RNA:DNA hybrids are involved in Ty1 multimer formation in *rrm3* mutants. Together, our findings suggest that Ty1 retrotransposition events containing RNA:DNA hybrid regions can function as replication fork blocks in *rrm3* mutants.

MATERIALS AND METHODS

Yeast strains: The genotypes of *S. cerevisiae* strains used in this study are listed in Table 1. All strains are derivatives of congenic strains BY4741 and BY4742 (Brachmann *et al.* 1998). Strain JC3212 contains the chromosomal Ty1*his3AI[Δ1]*-3114 element, which was introduced into strain BY4741 by galactose induction of the pGTy1*his3AI[Δ1]* element, as described previously (Curcio and Garfinkel 1991). Strains JC3900, JC3946, and JC3956 are spores derived from a cross between strain JC3212 and the *rtt101Δ::kanMX* derivative, the *rad51Δ::kanMX* derivative, or the *rad52Δ::kanMX* derivative of strain BY4742, respectively.

The *sgs1Δ::kanMX* allele in strain JC4915 and the *srs2Δ::kanMX* allele in strain JC4916 were each introduced by PCR-mediated gene disruption of strain JC3212 (Table 2). Gene replacements were confirmed by two independent PCR

TABLE 2

Oligonucleotide primers used in this study

Primer	Sequence
AD1	5′-NTCGASTWTSGWGTT-3′
AD2	5′-NGTCGASWGANAWGAA-3′
H3HOPA2	5′-TCTCCTACTTTCTCCCTTT GCAAACC-3′
HISOUT3	5′-CTTCGTTTATCTTGCCTGCTC-3′
PJ4	5′-ACCACTTGCGCTTATTTCTT GGAAGTGTTGTATCTCAAAAT GAGACTGTGCGGTATTTCACACCG-3′
PJ5	5′-ATGTTATTATAAACTACTTACCA AAAAAAGTGTTGTATTACGGGCAG ATTGTACTGAGAGTGCAC-3′
PJ37	5′-GACTGGGCCCGAATTCGACAG GTTATCAGCAAC-3′
PJ38	5′-TAGAAGTTCTCCTCGAGG AATAAG-3′
PJ111	5′-GTTTTTCTTCTTCAAGCACG TTAACCAG-3′
PJ143	5′-GATCTACCACCGCTCTGGA AAGTG-3′
TRPHOP-SE	5′-AGATTGTACTGAGAGTGCACC-3′
Ty1LTRF	5′-TCTTTGCCTTCGTTTATCTTGCCTG-3′
TyA1OUT	5′-CCTTAGAAGTAACCGAAGCA CAGGCG-3′
TyAOUT2	5′-TCTCTGGAACAGCTGATGAAG-3′
TyBOUT2	5′-GTGATGACAAAACCTCTTCCG-3′
U3SEQ	5′-GGCTATAATATTAGGTATACAG AATATACTAGAAGTTCTCCTC-3′

analyses. Oligomer sequences used to construct all deletion alleles and confirm gene replacements are available upon request. Strain JC4415 was constructed by introduction of the *rad52Δ::hisG-URA3-hisG* allele (Curcio and Garfinkel 1994) into strain JC3917. Strain JC5266 was constructed by two-step gene disruption of the *kanMX* gene that replaces the *RRM3* ORF in JC3917, followed by PCR-mediated introduction of the *rad51*::kanMX allele. Two-step gene disruption of *kanMX* was performed using plasmid pBJC934, which contains a *Xho*I–*Xba*I fragment of *kanMX* bearing an internal *Nsi*I deletion cloned into the *URA3*-based integrating vector, pRS406.

The *URA3-tG(GCC)B* locus in strains JC4522, JC4526, and JC4733 was constructed by insertion of the *URA3* gene 34 bp upstream of *tG(GCC)B* in strain BY4741 and the *rrm3ΔkanMX* and *ste12ΔkanMX* derivatives. The *URA3* gene was amplified from plasmid pRS406 DNA using oligomers PJ4 and PJ5.

Plasmids: Plasmid pGTy1*his3AI[Δ1]* was described previously (Scholes *et al.* 2001). The plasmid pOY1, a *URA3-CEN* vector carrying a Ty1*his3AI* element, was described in Lee *et al.* (1998). Plasmid pJC838 is a *LEU2-CEN* vector carrying *GAL1*p:Ty1*his3AI[Δ1]*. To construct pJC838, the *GAL1* promoter in plasmid pGTy1*his3AI[Δ1]* was amplified by PCR with oligomers PJ37 and PJ38. The PCR product was digested with *Apa*I and *Xho*I and cloned into pRS415 digested with *Apa*I and *Xho*I. The resulting plasmid, pBJC837, was digested with *Xho*I and *Eag*I, and the 7513-bp *Xho*I–*Eag*I fragment of pGTy1*his3AI[Δ1]* was inserted. The p*GAL1*:*RNH1* plasmid was a gift of Robert Crouch (National Institutes of Health). Plasmids pBDG542 (Curcio and Garfinkel 1994) and pJC573 (Bryk *et al.* 2001) were described previously.

Frequency of chromosomal Ty1*his3AI* element mobility: Cells from a single colony of each strain (JC3212, JC3917, JC3946, JC3956, JC4415, JC4915, JC4916, and JC5266) were grown to saturation in YPD broth at 30°, diluted 1:1000 into 8-ml YPD broth, divided into four cultures, and grown to saturation at 20°. Aliquots of each culture were plated on YPD agar and SC −His agar and the plates were incubated for 3 days at 30°, at which time colonies were counted.

PCR-based detection of multimeric cDNA arrays: Independent His$^+$ colonies that sustained an insertion of Ty1*HIS3* cDNA were obtained by spreading strains JC3212, JC3900, JC3917, JC4415, JC4915, and JC4916 on YPD agar. Following growth for 1 day at 30°, cells were replicated to YPD agar, grown at 20° for 3 days, and then replicated to SC −His agar and grown at 30°. His$^+$ papillae were single-colony purified. To test the effect of inducing the p*GAL1*:*RNH1* plasmid, strains JC3212, JC3917, and JC4915 transformed with plasmid pRS416 or p*GAL1*:*RNH1* were spread on SC −Ura agar and grown for 1 day at 30°. The lawns were replicated to YP agar containing 2% galactose and grown at 20° for 3 days. Subsequently, the lawns were replicated to SC −Ura −His agar to select His$^+$ isolates that had maintained the p*GAL1*:*RNH1* plasmid throughout the induction. His$^+$ papillae were single-colony purified.

Independent His$^+$ colonies were suspended in Lyse-N-Go PCR reagent (Pierce Chemical), according to the manufacturer's specifications. Cell suspensions were used as templates in PCR reactions with HISOUT3 and TyAOUT2 as primers. Isolates that yielded a band were retested by PCR using primers H3HOPA2 and TyA1OUT. Isolates that yielded a PCR product in both tests are included in Table 4 or Table 7. Several strains yielding products larger than predicted by the presence of two LTRs were subjected to DNA sequencing using primer HISOUT3. Differences between strains in the fraction of His$^+$ isolates harboring Ty1*HIS3*:Ty1 multimers were analyzed using Fisher's exact test (www.langsrud.com/fisher.htm). The two-tailed *P*-value is reported.

Rate of Ty1 integration at *URA3-tG(GCC)B* locus: Strains JC4522, JC4526, and JC4733 grown on SC −Ura agar were transferred to YPD broth and grown overnight at 30°. Each culture was diluted 1:1000 into YPD broth, and aliquoted into 1-ml cultures, which were grown to saturation at 20°. A 1-μl aliquot was removed from each of four cultures per strain and plated on YPD. Subsequently, each culture was plated on 5-FOA agar. The rate of FOA^r was determined from the median number of FOA^r colonies in 11 cultures divided by the average number of colonies in 4 cultures (Foster 2006). One independent FOA^r colony from each of 17 to 50 plates was single-colony purified. Following lysis of FOA^r colonies in Pierce Lyse-N-Go reagent, PCR reactions were performed with primers PJ111 and TRPHOP-SE, which generate a 1.4-kb band including the *URA3* ORF and promoter. In isolates lacking the 1.4-kb band, two subsequent PCR reactions using primer PJ111 and either TYA1OUT or TYBOUT2 were performed to confirm the presence of a Ty1 element in either orientation in *URA3*. In isolates in which the 1.4-kb band was shifted to 1.7 kb, two subsequent PCR reactions with primer U3SEQ and either PJ111 or TRPHOP-SE were performed to confirm the presence of a solo LTR within *URA3*.

Frequency of gene conversion of a Ty1*his3AI* element by Ty1*HIS3* cDNA: Plasmid pJC573, a *URA3* integrating vector that harbors Ty1*his3AI[Δ1]* upstream of the *BIK1-HIS4* intergenic region, was integrated into strain BY4741. The *rrm3Δ::kanMX*, *rad52Δ::kanMX*, and *rad27Δ::kanMX* alleles were subsequently introduced into a pJC573 integrant by PCR-mediated gene disruption. Following growth of each strain on YPD agar at 20°, independent His$^+$ Ura$^+$ isolates were obtained. The fraction of His$^+$ Ura$^+$ derivatives of each strain in which Ty1*HIS3* cDNA had replaced the Ty1*his3AI[Δ1]* allele was determined as described previously (Bryk *et al.* 2001).

TAIL PCR to identify the 3′ junction of Ty1*HIS3* cDNA with genomic DNA: Plasmid pOY1 was introduced into BY4741 and the *rrm3*Δ*::kanMX* derivative of BY4741. Large lawns of independent transformants were grown on SC −Ura agar overnight at 30°. The lawns were replicated to two YPD plates and each lawn was grown at 20° or 30° for 3 days. Lawns on YPD were replicated to SC −His agar and grown for 3 days at 30°. No His$^+$ colonies arose following growth on YPD agar at 30°, indicating that the His$^+$ colonies that arose following growth on YPD agar at 20° were independent. His$^+$ colonies were single-colony purified and replicated to FOA −His agar to select segregants lacking the pOY1 plasmid. Genomic DNA was isolated from His$^+$ Ura$^-$ isolates, and the 3′ junction between Ty1*HIS3* and genomic DNA was amplified by thermal asymmetric interlaced (TAIL) PCR (Liu and Whittier 1995). TAIL-PCR utilized each of three nested primers, H3HOPA2, PJ143, and HISOUT3 in successive reactions with an arbitrary degenerate primer (AD1 or AD2). Primary TAIL-PCR reaction mixtures contained 50 ng genomic DNA, primer H3HOPA2, and primer AD1 or AD2 in a 25-μl reaction. The product of the first reaction was diluted 1:20, and a 1-μl aliquot was used in a 25-μl PCR reaction containing primer PJ143 and primer AD1 or AD2. The secondary PCR reaction product was diluted 1:10, and 1 μl was used in a 25-μl PCR reaction containing primer HISOUT3 and AD1 or AD2. Thermal cycling conditions were those described previously (Liu and Whittier 1995) except that the annealing temperature varied between 62° and 67°, depending on the specific primer used. PCR products were visualized on a 1% agarose gel. If secondary and tertiary reactions yielded one major band, the tertiary reaction product was purified using the QIAquick PCR purification kit. If both the series of reactions with primer AD1 and the series of reactions with primer AD2 yielded a product, the larger of the two products was purified. Purified PCR products were cloned into the pCR2.1-TOPO vector using the InVitrogen TOPO TA cloning kit and sequenced. Sequences were compared to the Saccharomyces Genome Database (www.yeastgenome.org) to identify the Ty1*HIS3* insertion site.

CHEF gel analysis: Strains JC3212 was inoculated into 1 ml of YPD broth, while His$^+$ derivatives of strains JC3212, JC3917, and JC4915 were inoculated into 8 ml of SC −His broth, and the strains were grown overnight at 30°. Agarose-embedded chromosomal DNA was prepared from each culture (Gerring *et al.* 1991). Using a Biorad CHEF Mapper apparatus, samples were subject to electrophoresis on a 1% agarose gel in 0.5% TBE buffer at 6 V/cm for 24 hr. Pulse times of 45–120 sec were used to analyze native yeast chromosomes. The gels were stained with ethidium bromide and photographed. DNA from CHEF gels was transferred onto a Hybond-N+ membrane (Amersham), which was hybridized in NorthernMax buffer (Ambion) at 50° overnight with ^{32}P-labeled *HIS3* riboprobe synthesized using plasmid pGEM-HIS3 (Curcio *et al.* 1990).

RESULTS

Retromobility and formation of tandem Ty1 cDNA arrays are increased in *rrm3*Δ mutants: Considering that Sgs1, Rrm3, and Srs2 have partially overlapping functions in genome maintenance, and that the increased formation of cDNA multimers is correlated with increased retromobility in *sgs1*Δ mutants (Bryk *et al.* 2001), we compared the levels of Ty1 retromobility and multimer formation in *rrm3*Δ and *srs2*Δ mutants to that in *sgs1*Δ and wild-type strains. We used a chromosomal Ty1*his3AI* element to measure Ty1 retromobility (Curcio and Garfinkel 1991). The *his3AI* retrotranscript indicator gene consists of the *HIS3* gene interrupted by an artificial intron (AI) in antisense orientation. The *his3AI* gene is inserted in the 3′-UTR of a genomic Ty1 element in the opposing transcriptional orientation; consequently, splicing of AI from the Ty1*his3AI* RNA followed by reverse transcription of the spliced transcript generates Ty1 cDNA carrying a functional *HIS3* gene. When Ty1*HIS3* cDNA is incorporated into the genome by integration or by recombination with genomic Ty1 sequences, the cell becomes a His$^+$ prototroph. Therefore, the frequency of His$^+$ prototroph formation is a measure of the retromobility of the Ty1*his3AI* element. The frequency of Ty1*his3AI* retromobility was increased 42-fold in the *rrm3*Δ mutant (Table 3). This effect was substantially larger than that caused by *sgs1*Δ, which increased retromobility 12-fold. On the other hand, the *srs2*Δ mutation caused only a 3-fold increase in retromobility.

TABLE 3

Frequency of Ty1*his3AI* retromobility in DNA helicase mutants

Genotype	Frequency of Ty1*his3AI* retromobility[a] ± SE × 10^{-7}	Fold increase in the absence of *RRM3*, *SGS1*, or *SRS2*
WT	4.8 ± 0.3	1
*rrm3*Δ	204 ± 3	42
*sgs1*Δ	60.0 ± 2.9	12
*srs2*Δ	15.0 ± 0.8	3
*rad52*Δ	35.4 ± 0.5	1
*rad52*Δ *rrm3*Δ	66.6 ± 5.0	2
*rad51*Δ	18.0 ± 2.3	1
*rad51*Δ *rrm3*Δ	152 ± 20	8

[a] Ty1*his3AI* retromobility occurs when the Ty1*his3AI* RNA is spliced and reverse transcribed, and the resulting cDNA is incorporated into the genome by integration or recombination. The frequency of Ty1*his3AI* retromobility is the average of the number of His$^+$ prototrophs divided by the total number of cells plated for each of four cultures.

To measure the formation of Ty1 cDNA multimers in these strains, we isolated independent His$^+$ derivatives of strains containing a chromosomal Ty1*his3AI* element and used a PCR assay to detect Ty1*HIS3* cDNA that was a component of a multimeric Ty1 array (Figure 1). Using one primer that anneals to the splice junction in *HIS3* and another that anneals in *TYA1*, we detected junctions between the newly transposed Ty1*HIS3* element and a downstream Ty1 element containing a single LTR or two adjoining LTRs (Figure 1, A and B). In addition, irregular junctions with rearranged Ty1 sequences between adjoining elements were detected (Figure 1C). Each multimeric cDNA array that was detected contained at least two, but possibly more Ty1 cDNAs. In agreement with previous results in a different strain

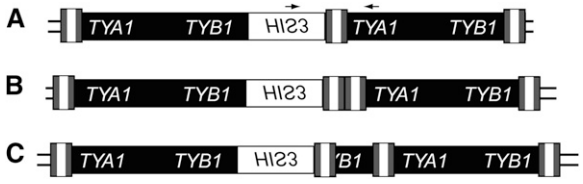

FIGURE 1.—Schematic of Ty1*HIS3*:Ty1 multimers. Simple Ty1 elements consist of LTRs (tripartite shaded and open rectangle) flanking a central coding region (solid rectangle) containing two open reading frames, *TYA1* and *TYB1*. The *HIS3* gene, which is in the opposite orientation relative to Ty1 ORFs, is represented by an open rectangle. (A) 1-LTR Ty1*HIS3*:Ty1 multimer. Primers used to detect all classes of Ty1*HIS3*:Ty1 multimers are represented by small arrows. (B) 2-LTR Ty1*HIS3*:Ty1 multimer. (C) A single representative of the diverse class of Ty1-*HIS3*:Ty1 multimers with irregular junctions (WEINSTOCK *et al.* 1990).

background (BRYK *et al.* 2001), 13% of independent His$^+$ derivatives of the wild-type strain were Ty1*HIS3*:Ty1 multimers (Table 4). Junctions containing one LTR were the most common, but 2-LTR junctions and irregular junctions were also observed. Deletion of *RRM3* or *SGS1* caused a significant increase in the fraction of Ty1*HIS3*:Ty1 multimers to 30% ($P < 0.001$) or 31% ($P < 0.01$) of total Ty1*HIS3* retromobility events, respectively. In contrast, deletion of *SRS2* caused only a minor increase in Ty1*HIS3*:Ty1 multimers. As in the wild-type strain, the majority of Ty1*HIS3*:Ty1 multimers in the *rrm3*Δ, *sgs1*Δ, and *srs2*Δ strains had 1-LTR junctions.

The homologous recombination protein, Rad52, is required for elevated retromobility and Ty1 multimer formation in *sgs1*Δ mutants (BRYK *et al.* 2001); therefore, we asked whether Rad52 is required in the *rrm3*Δ mutant. Ty1*his3AI* mobility was only twofold higher in the *rrm3*Δ *rad52*Δ mutant than in the *rad52*Δ mutant (Table 3). Thus, the *rrm3*Δ mutation causes increased Ty1 retromobility primarily by a Rad52-dependent mechanism. Furthermore, the fraction of Ty1*HIS3*:Ty1 multimers in the *rrm3*Δ *rad52*Δ mutant was reduced to 3%, which was significantly lower than that in the *rrm3*Δ mutant ($P < 0.01$; Table 4) and comparable to the fraction previously reported for a *rad52*Δ mutant (BRYK *et al.* 2001). Therefore, both increased retromobility and the formation of Ty1 cDNA arrays require Rad52 in the *rrm3*Δ mutant. We also examined the role of Rad51, which is required for gene conversion but not strand annealing, in retromobility. Retromobility was increased eightfold by deletion of *RRM3* in a *rad51*Δ mutant. Therefore, Rad51 is not critical for increasing retromobility of an *rrm3*Δ mutant.

To determine whether elevated Ty1 multimer formation is a general feature of mutants that have defects in replication fork progression, we also measured the fraction of Ty1*HIS3*:Ty1 multimers in an *rtt101*Δ mutant (Table 4). Like the *rrm3*Δ mutant, the *rtt101*Δ mutant has an elevated level of Ty1 cDNA and increased replication fork pausing at tRNA genes and other sites (LUKE *et al.* 2006; CURCIO *et al.* 2007). However, the fraction of Ty1*HIS3*:Ty1 multimers in an *rtt101*Δ mutant was equivalent to that in the wild-type strain. Therefore, Ty1 multimer formation is not elevated in all mutants that have increased replication fork pausing. Together, these findings implicate Ty1 multimer formation in the increased retromobility of *rrm3*Δ mutants as well as *sgs1*Δ mutants.

Neither integration nor recombination of Ty1 cDNA is substantially elevated in *rrm3*Δ mutants: To ascertain whether the formation of Ty1 cDNA multimers is a major cause of elevated retromobility in *rrm3*Δ mutants, we asked whether either cDNA integration or recombination of cDNA with genomic Ty1 elements was also elevated. First, we developed a quantitative assay for Ty1 integration upstream of a known hotspot, namely, the *tG(GCC)B* gene. This tRNA gene is the most strongly preferred target site for Ty1 among 16 different tRNA^{gly} genes in the genome. Furthermore, insertion of a *URA3* gene either 15 or 60 bases upstream of *tG(GCC)B* does not significantly alter the frequency of Ty1 integration (BACHMAN *et al.* 2004). Therefore, we introduced the *URA3* gene 34 bp upstream of *tG(GCC)B*, in the same transcriptional orientation, and measured the rate of Ty1 insertion into *URA3* (Figure 2). The rate of Ty1 insertion upstream of *tG(GCC)B* is the product of the rate of FOA^r and the fraction of independent FOA^r colonies in which Ty1 had integrated into *URA3*. Integration of Ty1 in either orientation was detected by

TABLE 4

Ty1*HIS3*:Ty1 multimer formation in His$^+$ isolates

Genotype	1-LTR Ty1*HIS3*:Ty1 multimer/His$^+$ isolate (%)	2-LTR Ty1*HIS3*:Ty1 multimer/His$^+$ isolate (%)	Irregular Ty1*HIS3*:Ty1 multimer/His$^+$ isolate (%)	Total Ty1*HIS3*:Ty1 multimers/His$^+$ isolate (%)
WT	13/188 (7)	7/188 (4)	4/188 (2)	24/188 (13)
*rrm3*Δ	46/213 (22)	5/213 (2)	13/213 (6)	64/213 (30)
*sgs1*Δ	27/102 (26)	3/102 (3)	2/102 (2)	32/102 (31)
*srs2*Δ	21/143 (15)	4/143 (3)	1/143 (2)	26/143 (18)
*rtt101*Δ	6/64 (9)	3/64 (5)	0/64 (0)	9/64 (14)
*rrm3*Δ *rad52*Δ	1/32 (3)	0/32 (0)	0/32 (0)	1/32 (3)

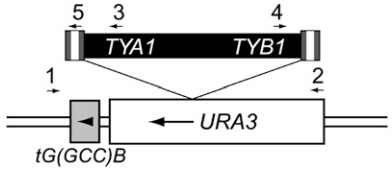

FIGURE 2.—Integration of a Ty1 element into the *URA3-tG(GCC)B* locus. The *URA3* gene was inserted 34 bp upstream of the *tG(GCC)B* gene. FOA^r colonies were screened by PCR using primers that flank the locus (denoted by arrows 1 and 2) to detect the presence of an insertion within the *URA3* gene. Subsequent PCR reactions using primers 1 and 3 or 1 and 4 were performed to detect the specific presence of a Ty1 element. In the case of a 0.3-kb insertion into *URA3*, PCR reactions using primers 1 and 5 and 2 and 5 were performed to detect solo LTR insertions.

PCR (Figure 2). Retrotransposition into *URA3-tG(GCC)B* occurred at a rate of 1.9×10^{-7} per generation in the wild-type strain (Table 5). This rate was reduced at least 200-fold by deletion of the gene encoding the Ty1 transcription factor, Ste12, confirming that Ty1 integration is a major cause of *URA3* inactivation. While the rate of FOA^r increased modestly in the *rrm3*Δ mutant, the fraction of Ty1 insertions into *URA3* decreased, resulting in nearly equivalent rates of Ty1 integration into *URA3-tG(GCC)B* in the wild-type and *rrm3*Δ strains (Table 5). This result is consistent with our previous finding in a study that employed a semi-quantitative PCR assay to detect Ty1 integration upstream of all 16 tRNA^{gly} genes (SCHOLES *et al.* 2001). Therefore, the *rrm3*Δ mutation does not increase integration into preferred target sites.

Alternatively, Ty1 cDNA may be incorporated into the genome of *rrm3*Δ mutants by recombination with genomic Ty1 elements. To test this idea, we measured the frequency of gene conversion of a chromosomal Ty1*his3AI* element by Ty1*HIS3* cDNA using a previously described genetic assay (BRYK *et al.* 2001). *RRM3*, *RAD52*, and *RAD27* were deleted from a strain containing 1.2-kb direct repeats of the *BIK1-HIS4* intergenic region flanking a Ty1*his3AI* element and the *URA3* gene. Independent His$^+$ Ura$^+$ derivatives of each strain were selected. His$^+$ Ura$^+$ isolates that became His$^-$ as a result of selection for the loss of *URA3* were scored as recombinants formed through gene conversion of Ty1*his3AI* by Ty1*HIS3* cDNA. The frequency of cDNA recombination with Ty1*his3AI* in the wild-type strain was 1.3% (Table 6). The frequency was threefold lower in the recombination-defective *rad52*Δ mutant and twofold higher in the *rad27*Δ mutant, which has previously been reported to have an elevated level of Ty1 cDNA recombination (SUNDARARAJAN *et al.* 2003). However, deletion of *RRM3* had no effect on the frequency of cDNA recombination in our assay.

TABLE 5

Ty1 retrotransposition into the *URA3-tG(GCC)B* locus

Genotype	Rate of FOA^r ± SE ($\times 10^{-7}$)	Ty1 or solo LTR integrants in *URA3*[a]/no. of FOA^r colonies	Rate of Ty1 integration upstream of *tG(GCC)B* ($\times 10^{-7}$)
WT	2.5 ± 0.8	37/50	1.9
*rrm3*Δ	10.2 ± 2.9	8/27	3.0
*ste12*Δ	<0.04	4/17	<0.009

[a] As determined by the PCR assays described in Figure 2. Two isolates with a solo LTR in *URA3*, presumably the product of Ty1 integration followed by recombination between the LTRs, were identified in the wild-type strain background.

TABLE 6

Recombination between Ty1*HIS3* cDNA and a genomic Ty1*his3AI* element

Genotype	No. of His$^-$ Ura$^-$ recombinants/no. of His$^+$ Ura$^+$ isolates (%)
WT	10/758 (1.3)
*rad52*Δ	3/672 (0.4)
*rad27*Δ	25/902 (2.8)
*rrm3*Δ	9/799 (1.1)

An independent method was used to explore the possibility that Ty1 cDNA integration at novel target sites, or cDNA recombination with other genomic Ty1 sequences such as solo LTRs, contributes to elevated retromobility in the absence of Rrm3. Sites of Ty1*HIS3* insertion into the genome were identified by TAIL-PCR followed by sequencing of the PCR products. To perform this analysis, a Ty1*his3AI* element on a *CEN*-based vector was introduced into strain BY4741 and the isogenic *rrm3*Δ strain. Fifteen independent His$^+$ derivatives of strain BY4741 and 41 His$^+$ derivatives of the *rrm3*Δ mutant were isolated. After segregation of the Ty1*his3AI* donor plasmid, genomic DNA was isolated and used as a template in TAIL-PCR to amplify genomic sequences adjacent to the 3′-LTR of the Ty1*HIS3* element. In the *rrm3*Δ mutant, 10 of the 41 TAIL-PCR products (24%) contained *TYA1* sequences immediately downstream of the Ty1*HIS3* LTR, consistent with the presence of Ty1*HIS3* cDNA in a dimeric array with a 1-LTR junction (see supporting information, Table S1 A). Three other TAIL-PCR products contained the junction between the 3′ end of Ty1*HIS3* and sequences within a Ty1, Ty2, or Ty4 LTR at a genomic location that could not be determined due to the short length of the TAIL-PCR products (Table S1 B). Of the remaining 28 events, none of the Ty1*HIS3* LTR:genomic DNA junctions was at a preexisting LTR:genomic DNA junction. Therefore, gene conversion of genomic Ty1 sequences by Ty1*HIS3* cDNA accounted for <4% of Ty1*HIS3* mobility events in the *rrm3*Δ mutant. Furthermore, the specificity of Ty1 integration in the *rrm3*Δ mutant was

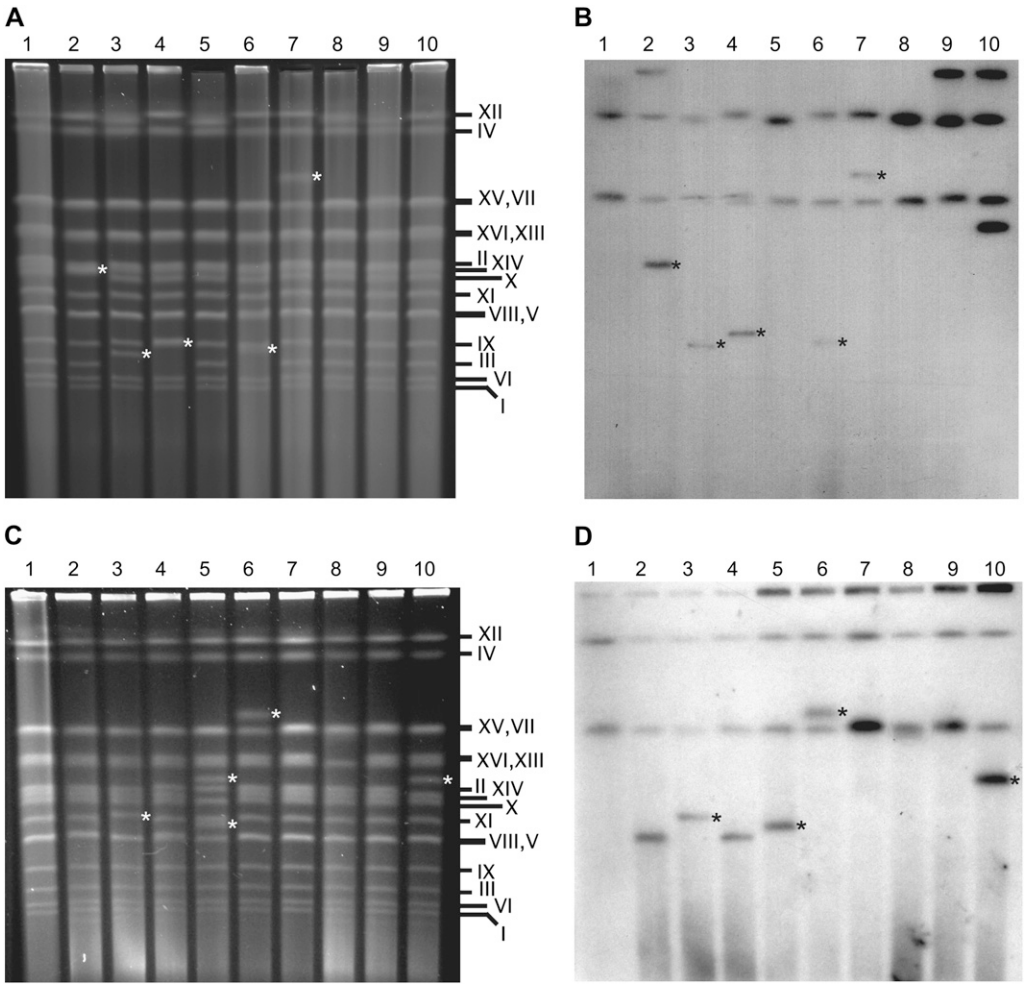

FIGURE 3.—Ty1*HIS3*:Ty1 multimers are located on chromosomes that have undergone rearrangement. (A) Intact chromosomes separated by CHEF gel electrophoresis. Lane 1, the His$^-$ wild-type strain, JC3212; lanes 2–10, His$^+$ derivatives of the isogenic *rrm3*Δ strain, JC3917, harboring a 1-LTR Ty1*HIS3*:Ty1 multimer. (B) Southern blot of the gel in A probed with *HIS3*. (C) CHEF analysis of intact chromosomes. Lane 1, the His$^-$ wild-type strain JC3212; lanes 2–10, His$^+$ derivatives of the isogenic *sgs1*Δ strain, JC4915, harboring a 1-LTR Ty1*HIS3*:Ty1 multimer. The His$^+$ isolate in lane 5 is the only one in which two rearranged chromosomes were detected. (D) Southern blot of the gel in C probed with *HIS3*. White asterisks in A and C indicate new chromosome bands. In B and D, bands that correspond to novel chromosome bands in A and C are marked with a black asterisk. The *his3*Δ*1* allele present in every strain is located on chromosome XV. The Ty1*his3AI*-3114 element present in every strain is located on chromosome XII.

similar to that in a wild-type strain. In 24 of 28 *rrm3*Δ isolates (86%), Ty1*HIS3* integrated within an 825-bp window upstream of a gene transcribed by RNA polymerase III. This window is a well-characterized hotspot for Ty1 integration (DEVINE and BOEKE 1996; BACHMAN *et al.* 2004). In 1 of 28, Ty1*HIS3* integrated downstream of a tRNA gene, while in 3 others, Ty1*HIS3* integrated between two divergently transcribed open reading frames. Bidirectional promoter regions have not previously been described as preferred sites of Ty1 integration, raising the possibility that they become stronger targets in the absence of Rrm3.

In comparison to 10 of 41 Ty1*HIS3* insertions in the *rrm3*Δ mutant, none of 15 Ty1*HIS3* insertions was present as a Ty1*HIS3*:Ty1 multimer in the wild-type strain (Table S1 C). In 3 of 15, Ty1*HIS3* integrated into a Ty1 or Ty4 LTR at an undetermined genomic location. In the remaining 12, the upstream regions of genes transcribed by RNA polymerase III were targeted 11 times (92%), while one Ty1*HIS3* element integrated into the *CHK1* open reading frame, which is not in the vicinity of an RNA polymerase III transcription unit. We conclude that neither gene conversion of Ty1 elements by Ty1 cDNA nor a greatly expanded integration target range is a major factor in the elevated Ty1 cDNA mobility in *rrm3* mutants. Since the rate of Ty1 integration into a preferred target is also not increased (Table 5), it is likely that most of the Ty1 cDNA in *rrm3* mutants is inserted into the genome in multimeric arrays.

We analyzed the 28 *rrm3* His$^+$ isolates with characterized Ty1*HIS3*:genomic DNA junctions (Table S1 B) by Southern analysis and by PCR to determine whether the integrated Ty1*HIS3* element was part of a Ty1 multimer. None of these 28 integration events were multimeric (data not shown). This finding suggests that when Ty1*HIS3* cDNA is incorporated into a multimer, it is rarely if ever present at the 3′ junction with genomic DNA. Therefore, we cannot use genomic insertion site data to determine whether Ty1 multimers are present at sites of integration into the genome or recombination with the genome.

Ty1 cDNA multimers are associated with chromosomal rearrangements: Tandem arrays of Ty1 elements have been found at chromosomal breakpoint junctions,

TABLE 7

Chromosomal rearrangements in His$^+$ isolates

Genotype	Fraction of His$^+$ isolates with a chromosomal rearrangement[a]				
	Nonmultimeric Ty1*HIS3* (%)	1-LTR Ty1*HIS3*:Ty1 multimer (%)	2-LTR Ty1*HIS3*:Ty1 multimer (%)	Irregular Ty1*HIS3*:Ty1 multimer (%)	Total Ty1*HIS3*:Ty1 multimers (%)
WT	0/30 (0)	3/10 (30)	0/5 (0)	1/3 (33)	4/18 (22)
*rrm3*Δ	1/34 (3)	16/34 (47)	0/3 (0)	1/8 (13)	17/45 (38)
*sgs1*Δ	1/18 (6)	8/23 (35)	0/3 (0)	0/1 (0)	8/27 (30)

[a] Chromosome bands of a novel size relative to the wild-type strain prior to selection for Ty1*HIS3* retromobility.

suggesting that cDNA multimers can form during chromosomal break repair (Umezu *et al.* 2002; Maxwell and Curcio 2007b). To determine whether there is a connection between Ty1 multimer formation and chromosomal break repair in *rrm3*Δ mutants, we asked whether isolates containing Ty1*HIS3*:Ty1 multimers have an increased incidence of chromosomal rearrangements. The chromosomal banding pattern of His$^+$ isolates with or without a Ty1*HIS3*:Ty1 multimer (Table 4) was analyzed using clamped homogeneous electric field (CHEF) gels. Chromosome bands with a novel migration position in His$^+$ isolates relative to the bands in a wild-type His$^-$ strain (prior to Ty1*his3AI* transposition) were scored as chromosomal rearrangements (Figure 3). In the wild-type strain, 4 of 18 His$^+$ isolates with a Ty1*HIS3*:Ty1 multimer (22%) harbored one chromosomal rearrangement (Table 7). In contrast, no chromosomal rearrangements were observed in 30 His$^+$ isolates that had a nonmultimeric Ty1*HIS3* insertion (0%), which is a significantly lower percentage ($P < 0.05$). In the *rrm3*Δ mutant, 38% of isolates with a Ty1*HIS3*:Ty1 multimer had a chromosomal rearrangement compared to 3% of isolates with a monomeric Ty1*HIS3* insertion ($P < 0.01$). The percentage of *rrm3*Δ isolates with chromosomal rearrangements was even higher (47%) when only those harboring 1-LTR Ty1*HIS3*:Ty1 multimers were considered. In the *sgs1*Δ strain, His$^+$ isolates with multimeric Ty1*HIS3*:Ty1 insertions also had markedly higher levels of chromosomal rearrangements compared to isolates with monomeric Ty1*HIS3* insertions (30 and 6%, respectively). Together, the data in Table 7 suggest that a substantial fraction of isolates with Ty1 cDNA multimers, particularly 1-LTR multimers, are associated with chromosomal rearrangements in a wild-type strain, and this fraction is increased when either *SGS1* or *RRM3* is deleted.

If Ty1*HIS3*:Ty1 multimers form at chromosomal breakpoints, we would expect to find the Ty1*HIS3* cDNA on the rearranged chromosome. We performed Southern blot analysis of chromosomal DNA from 3 wild-type, 14 *rrm3*Δ, and 7 *sgs1*Δ isolates that harbored a 1-LTR Ty1*HIS3*:Ty1 multimer as well as a chromosomal band of a novel size. *HIS3* was located on a novel chromosome band in all 24 isolates (Figure 3 and data not shown). Together, these findings provide evidence that 1-LTR Ty1 multimers form at chromosomal break sites in all three of the strains, whereas monomeric Ty1 integration events are significantly less likely to occur at breakpoints.

Expression of RNase H suppresses Ty1 multimer formation but not retromobility in an *rrm3* mutant: Insertion of multimeric Ty1 cDNA could occur during repair of chromosomal breaks at two different types of sites in the *rrm3*Δ mutant. The first type comprises sites occupied by nonnucleosomal protein:DNA complexes, which are common features of the sites where replication pausing and chromosomal breaks occur in the *rrm3* mutant (Ivessa *et al.* 2000, 2002, 2003). The second type comprises RNA:DNA hybrid regions, which are proposed to be substrates of the Rrm3 helicase (Boule and Zakian 2006). Immediately following integration, Ty1 cDNA could contain RNA:DNA hybrid regions resulting from incomplete reverse transcription (Muller *et al.* 1991). If retrotransposition occurs prior to replication, Rrm3 could be required to traverse these regions. To test the idea that Ty1 cDNA multimers form at breaks initiated by RNA:DNA hybrids, we expressed a cellular RNase H, encoded by the *RNH1* gene, from the inducible *GAL1* promoter to degrade the RNA strand of RNA:DNA hybrids. The p*GAL1-RNH1* plasmid was expressed in an *rrm3*Δ, *sgs1*Δ, or wild-type strain harboring Ty1*his3AI*, and the effects on Ty1 retromobility and Ty1 multimer formation were determined. Notably, expression of p*GAL1:RNH1* had no effect on the level of Ty1 retromobility in a wild-type, *rrm3*Δ, or *sgs1*Δ strain (see Figure S1), suggesting that it did not interfere with the synthesis of Ty1 cDNA in cytoplasmic VLPs. However, expression of p*GAL1:RNH1* completely suppressed Ty1*HIS3*:Ty1 multimer formation in the *rrm3*Δ mutant ($P < 0.05$), such that the level of Ty1*HIS3*:Ty1 multimers in the *rrm3*Δ mutant with RNase H expression was as low as the level of Ty1 multimers in the wild-type strain without p*GAL1:RNH1* (Table 8). In contrast, expression of p*GAL1:RNH1* did not alter the fraction of Ty1*HIS3* mobility events that were multimeric in a wild-type strain or an *sgs1*Δ mutant. Therefore, RNA:DNA hybrid regions in the chromosome are likely to trigger the formation of Ty1 cDNA multimers specifically in the absence of Rrm3.

TABLE 8

Effect of RNase H overexpression on Ty1*HIS3*:Ty1 multimer formation

Genotype	Plasmid	1-LTR Ty1*HIS3*:Ty1 multimer/His$^+$ isolate (%)	2-LTR Ty1*HIS3*:Ty1 multimer/His$^+$ isolate (%)	Irregular Ty1*HIS3*:Ty1 multimer/His$^+$ isolate (%)	Total Ty1*HIS3*:Ty1 multimers/His$^+$ isolate (%)
WT	Vector	9/68 (13)	2/68 (3)	0/68 (0)	11/68 (16)
WT	p*GAL1*:*RNH1*	6/58 (10)	4/58 (7)	1/58 (2)	11/58 (19)
*rrm3*Δ	Vector	14/56 (25)	3/56 (5)	2/56 (4)	19/56 (34)
*rrm3*Δ	p*GAL1*:*RNH1*	4/56 (7)	0/56 (0)	1/56 (2)	5/56 (9)
*sgs1*Δ	Vector	12/66 (18)	2/66 (3)	3/66 (5)	17/66 (26)
*sgs1*Δ	p*GAL1*:*RNH1*	16/66 (24)	0/66 (0)	2/66 (3)	18/66 (27)

DISCUSSION

DNA helicases act on a variety of substrates to carry out their diverse functions in the cell. Not only do they unwind double-stranded DNA, but they also unwind RNA:DNA hybrids (Shin and Kelman 2006; Boule and Zakian 2007) and remove protein from single-stranded DNA (Krejci *et al.* 2003; Veaute *et al.* 2003; Byrd and Raney 2004). Members of the Pif1 family of DNA helicases function in the maintenance of mitochondrial and nuclear genomes, but the precise nature of their substrates is an important and unresolved issue. *S. cerevisiae* has two members of this family, Pif1 and Rrm3, which have distinct functions in the cell (Ivessa *et al.* 2000). Both helicases have been implicated in the removal of protein complexes from DNA and in the unwinding of RNA:DNA hybrid regions (Ivessa *et al.* 2003; Boule *et al.* 2005; Boule and Zakian 2006, 2007). In this work, we explored the role of Rrm3 in repressing Ty1 retromobility. We found that formation of Ty1 cDNA multimers is a major pathway of retromobility in *rrm3* mutants and that there is a significant correlation between cDNA multimers and chromosomal rearrangements. Moreover, Ty1 multimer formation in an *rrm3* mutant is suppressed by the overexpression of RNase H. Together, these results suggest that RNA:DNA hybrid regions in nascent retrotransposition events are substrates of the Rrm3 helicase.

Ty1 cDNA levels are significantly elevated in the absence of Rrm3, in part because Ty1 cDNA synthesis is stimulated through the DNA damage checkpoint pathway (Scholes *et al.* 2001; Curcio *et al.* 2007). Despite the elevated levels of cDNA, deletion of *RRM3* does not increase integration into a preferred target, namely the region upstream of tRNA genes (Table 5; see also Scholes *et al.* 2001). Furthermore, target-site specificity of Ty1 is similar in the presence and absence of Rrm3 (Table S1). Thus, increased recombination of Ty1 cDNA rather than elevated levels of integration may underlie the higher levels of retromobility in the absence of Rrm3. Consistent with this idea, we found only a twofold increase in retromobility when *RRM3* was deleted in a *rad52*Δ strain (Table 3). However, three observations suggest that Ty1 cDNA is rarely a donor for gene conversion of genomic Ty1 sequences in the *rrm3* mutant. First, Rad51, which is required for gene conversion, is not required for the increase in retromobility that results from deletion of *RRM3*. Second, gene conversion of a chromosomal Ty1*his3AI* element by its cDNA was not elevated in the absence of Rrm3 (Table 6). Third, gene conversion of 1 of the 32 Ty1 elements or 185 Ty1 LTRs in the *S. cerevisiae* genome (Kim *et al.* 1998) by Ty1*HIS3* cDNA was not observed in the analysis of 41 Ty1*HIS3* insertion sites in the *rrm3*Δ mutant, even though 12 of the 41 Ty1*HIS3* insertions sites resulted from integration into Ty LTRs (Table S1). On the other hand, the formation of multimeric Ty1 cDNA arrays was significantly increased in the *rrm3* mutant. Most of the multimers had one LTR at the junction between cDNAs, implicating the involvement of homologous recombination between LTRs of individual cDNAs in their formation. Together, our results point to Ty1 multimer formation as a major route of Ty1 retromobility in the *rrm3*Δ mutant. Multimer formation results in higher levels of retromobility by increasing the average number of cDNA molecules that are incorporated into the genome of each cell that sustains a retromobility event, rather than by increasing the proportion of cells in which cDNA is inserted. Interestingly, multimer formation is not a mandatory pathway for cDNA insertion in the *rrm3* mutant, since cDNA can be incorporated via alternative pathways, such as integration, when multimer formation is blocked. For example, deletion of *RAD52* in an *rrm3* mutant resulted in only a small reduction in the level of retromobility. (Compare the retromobility frequency in the *rrm3*Δ mutant to the *rrm3*Δ *rad52*Δ mutant in Table 3.) Similarly, overexpression of RNase H suppressed the formation of Ty1 multimers in an *rrm3* mutant without affecting the frequency of Ty1 retromobility.

The frequency of Ty1 multimer formation is similar between *rrm3*Δ and *sgs1*Δ mutants (Table 4), but the frequency of Ty1*his3AI* retromobility is substantially higher in an *rrm3*Δ mutant. We cannot yet explain this discrepancy, but it could be due to a higher average

number of monomeric units within cDNA arrays in an *rrm3*Δ mutant relative to the *sgs1*Δ mutant. The fact that the *rrm3*Δ mutant has more Ty1 cDNA per cell than the *sgs1*Δ mutant supports this idea (Bryk *et al.* 2001; Scholes *et al.* 2001).

We have observed that the presence of chromosomal rearrangements, which could be large insertions or translocations, is correlated with the formation of multimeric Ty1 cDNA arrays in the *rrm3*Δ mutant as well as in the *sgs1*Δ mutant and the wild-type strain. This correlation is even stronger when only 1-LTR multimers are considered (Table 7). Moreover, in isolates that harbor both a 1-LTR multimer and a rearrangement, the *HIS3*-marked multimer is found on the rearranged chromosome (Figure 3 and data not shown). Together, these observations suggest that Ty1 multimers are frequently formed at chromosomal break sites. Notably, the fraction of multimer-containing isolates that harbor a chromosomal rearrangement is lowest in the wild-type strain, intermediate in the *sgs1* strain, and highest in the *rrm3* mutant (Table 7). Perhaps this observation reflects the fact that most rearrangements are large insertions of cDNA arrays, which would have to contain at least six or seven Ty1 cDNAs to cause a chromosomal band shift that is large enough to detect by CHEF gel analysis. Thus, the level of Ty1 cDNA, which is lowest in the wild-type strain and highest in the *rrm3* mutant, may directly influence the fraction of Ty1 cDNA multimers that are large enough to be detected as rearrangements in each strain. His^+ isolates of the *rrm3*Δ mutant can harbor Ty1 arrays consisting of as many as 25 cDNA monomers (data not shown), which are certainly long enough to result in a chromosomal band shift.

We took advantage of the fact that overexpression of a cellular RNase H does not inhibit the level of Ty1 retromobility in the wild-type, *rrm3*, or *sgs1* strain to ask whether the presence of an RNA:DNA hybrid promotes the formation of Ty1 multimers. Despite the association of Ty1 multimers with chromosomal breaks in all three strains, overexpression of RNase H suppressed multimer formation only in the *rrm3* mutant, and not in the wild-type or *sgs1*Δ strain (Table 8). This result strongly suggests that RNA:DNA hybrids promote multimer formation specifically in the *rrm3* mutant. Other types of DNA lesions may be involved in initiating multimer formation in the wild-type strain and the *sgs1* mutant.

How are multimeric arrays of Ty1 cDNAs incorporated into the genome in an *rrm3*Δ mutant? A model for these events must take into account the significant association between Ty1 multimers and genome rearrangements and the requirement for RNA:DNA hybrids in the increase in multimer formation in the *rrm3*Δ mutant. Our evidence favors a model in which Ty1 cDNA containing internal RNA:DNA hybrid regions is integrated into the genome prior to replication (Figure 4A). The presence of an RNA:DNA hybrid, which results from incomplete synthesis of the plus strand of cDNA, has been observed in the nucleic acids of Ty1 VLPs (Muller *et al.* 1991). If the RNA:DNA hybrid cannot be traversed by the replication fork in the absence of Rrm3 (Figure 4B), it could trigger the formation of a chromosome break within Ty1 sequences. The broken DNA end could then recombine with an extragenomic Ty1 cDNA molecule. Once one cDNA is incorporated at the break site, its free LTR end could recombine with the LTR of another extragenomic cDNA molecule, forming an array with 1-LTR at the junction. Subsequent recombination-mediated incorporation of cDNA at the break site would increase the size of the multimeric cDNA array. These recombination events could occur by strand annealing, consistent with the requirement for Rad52 but not for Rad51. Eventually, the chromosome end would be repaired by recombination with a genomic Ty1 element (Figure 4C), resulting in formation of a rearranged chromosome (Figure 4D). The genomic element with which the broken end recombines could be the newly retransposed element on the sister chromatid, or an ectopic Ty1 element. This model predicts that multimeric cDNA arrays and chromosomal rearrangements form at sites of retrotransposition, and thus, explains why a high level of chromosomal rearrangement is seen specifically when multimeric retromobility events are selected (Table 7). This model also provides an explanation for the low level of recombination between Ty1*HIS3* cDNA and genomic Ty1 elements in the *rrm3* mutant, since the breaks that are repaired by Ty1 cDNA occur at nascent sites of retrotransposition, rather than at Ty1 elements preexisting in the genome.

It has previously been proposed that Rrm3 is required for replication through nonnucleosomal protein-DNA complexes rather than RNA:DNA hybrids (Ivessa *et al.* 2003). This putative role is not necessarily conflicting with our observation that RNA:DNA hybrids trigger Ty1 cDNA multimer formation in the *rrm3*Δ mutant. Perhaps it is not the RNA:DNA hybrid *per se* that stalls the replication fork in *rrm3* mutants, but instead the presence of a protein that is specifically bound to this region. If so, one possible protein that could be bound to the RNA:DNA hybrid region within nascent retrotransposition events is the Ty1 reverse transcriptase. Reverse transcription of the double-strand Ty1 cDNA may be a very inefficient process (Muller *et al.* 1991); therefore, it is conceivable that reverse transcriptase remains bound to the RNA:DNA hybrid regions in nascent retrotransposition events.

Two alternative models for the formation of Ty1 multimers in *rrm3* mutants cannot be eliminated by the data presented but are considered unlikely. The first is that Ty1 cDNA forms multimeric arrays by homologous recombination prior to its incorporation into the genome by integration. If Ty1 arrays in the genome are refractory to progression of the replication fork, they could give rise to chromosomal rearrangements. In this

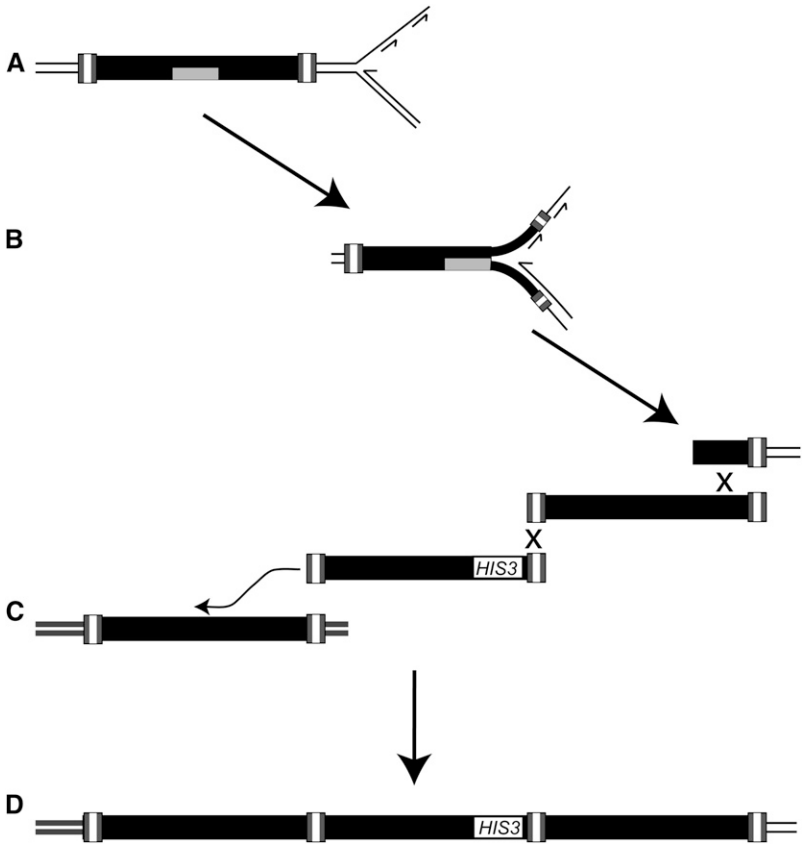

FIGURE 4.—A model for the formation of Ty1 cDNA multimers in *rrm3* mutants, and their association with chromosomal rearrangements. (A) Ty1 retrotransposition is proposed to occur directly before replication, resulting in incorporation of RNA (shaded rectangle):DNA hybrids into the genome. (B) The RNA:DNA hybrids function as replication fork blocks that give rise to a chromosome break in the absence of Rrm3. (C) The broken chromosomal fragment recombines with multiple copies of extrachromosomal Ty1 cDNA (illustrated by an "X") prior to recombination with the Ty1 element on the sister chromatid or with an ectopic copy of Ty1 (illustrated by the curved arrow). (D) These events result in a multimeric Ty1 cDNA array at a chromosomal breakpoint junction.

model, Rrm3 might repress Ty1 multimer formation by unwinding RNA:DNA heteroduplexes in Ty1 cDNA so that the cDNA can be repaired, thereby preventing its use as a substrate for multimer formation. It is important to note however, that this model invokes a role for Rrm3 outside of replication, which is inconsistent with studies showing its involvement in replication fork progression (SCHMIDT *et al.* 2002; AZVOLINSKY *et al.* 2006; MATSUDA *et al.* 2007).

The second alternative is that following a chromosomal break at a stalled replication fork in the *rrm3* mutant, the ends are resected until Ty1 sequences are reached. Subsequently, the chromosome end would recombine with multiple Ty1 cDNAs before recombining with the allelic Ty1 sequences on the sister chromatid or with an ectopic Ty1 element. The high levels of chromosomal breaks in *rrm3* mutants render this an appealing model. However, the model does not provide an obvious rationale for the role of RNA:DNA hybrids in Ty1 multimer formation and is inconsistent with several observations. First, chromosomal rearrangements are rare in the absence of selection for retromobility events, despite the high level of chromosomal breaks in an *rrm3* mutant (IVESSA *et al.* 2003; SCHMIDT and KOLODNER 2006). Second, gene conversion of genomic Ty1 elements or LTRs by cDNA occurs rarely in *rrm3* mutants (Table 6 and Table S1), whereas this model predicts that gene conversion events would be common. Third, no increase in Ty1 multimer formation was observed in an *rtt101*Δ mutant, even though this mutant also has an elevated level of replication fork stalling. In contrast, this model predicts that other mutants with increased replication fork pausing might also have higher levels of Ty1 multimers.

The results presented here raise the possibility that retrotransposition occurs shortly before replication, precluding repair of the RNA:DNA hybrid before the replication fork passes through the newly transposed element. This idea is supported by previous findings that retrotransposition is inhibited by arresting yeast cells in G1 and stimulated by prolonging S phase with hydroxyurea (XU and BOEKE 1991; CURCIO *et al.* 2007). This mode of retrotransposition is optimal for the spread of the retrotransposon, since it results in the presence of the replicated retrotransposon in both the mother and daughter cells.

We are grateful to Suzanne Sandmeyer for comments on the manuscript and to the Wadsworth Applied Genomic Technologies Core for DNA sequencing. This work was supported by National Institutes of Health grant GM52072.

LITERATURE CITED

AZVOLINSKY, A., S. DUNAWAY, J. Z. TORRES, J. B. BESSLER and V. A. ZAKIAN, 2006 The S. cerevisiae Rrm3p DNA helicase moves with the replication fork and affects replication of all yeast chromosomes. Genes Dev. **20:** 3104–3116.

Bachman, N., Y. Eby and J. D. Boeke, 2004 Local definition of Ty1 target preference by long terminal repeats and clustered tRNA genes. Genome Res. **14:** 1232–1247.

Boule, J. B., L. R. Vega and V. A. Zakian, 2005 The yeast Pif1p helicase removes telomerase from telomeric DNA. Nature **438:** 57–61.

Boule, J. B., and V. A. Zakian, 2006 Roles of Pif1-like helicases in the maintenance of genomic stability. Nucleic Acids Res. **34:** 4147–4153.

Boule, J. B., and V. A. Zakian, 2007 The yeast Pif1p DNA helicase preferentially unwinds RNA DNA substrates. Nucleic Acids Res. **35:** 5809–5818.

Brachmann, C. B., A. Davies, G. J. Cost, E. Caputo, J. Li *et al.*, 1998 Designer deletion strains derived from Saccharomyces cerevisiae S288C: a useful set of strains and plasmids for PCR-mediated gene disruption and other applications. Yeast **14:** 115–132.

Bryk, M., M. Banerjee, D. Conte, Jr. and M. J. Curcio, 2001 The Sgs1 helicase of Saccharomyces cerevisiae inhibits retrotransposition of Ty1 multimeric arrays. Mol. Cell. Biol. **21:** 5374–5388.

Byrd, A. K., and K. D. Raney, 2004 Protein displacement by an assembly of helicase molecules aligned along single-stranded DNA. Nat. Struct. Mol. Biol. **11:** 531–538.

Curcio, M. J., and D. J. Garfinkel, 1991 Single-step selection for Ty1 element retrotransposition. Proc. Natl. Acad. Sci. USA **88:** 936–940.

Curcio, M. J., and D. J. Garfinkel, 1994 Heterogeneous functional Ty1 elements are abundant in the *Saccharomyces cerevisiae* genome. Genetics **136:** 1245–1259.

Curcio, M. J., A. M. Hedge, J. D. Boeke and D. J. Garfinkel, 1990 Ty RNA levels determine the spectrum of retrotransposition events that activate gene expression in Saccharomyces cerevisiae. Mol. Gen. Genet. **220:** 213–221.

Curcio, M. J., A. E. Kenny, S. Moore, D. J. Garfinkel, M. Weintraub *et al.*, 2007 S-phase checkpoint pathways stimulate the mobility of the retrovirus-like transposon Ty1. Mol. Cell. Biol. **27:** 8874–8885.

Devine, S. E., and J. D. Boeke, 1996 Integration of the yeast retrotransposon Ty1 is targeted to regions upstream of genes transcribed by RNA polymerase III. Genes Dev. **10:** 620–633.

Fabre, F., A. Chan, W. D. Heyer and S. Gangloff, 2002 Alternate pathways involving Sgs1/Top3, Mus81/ Mms4, and Srs2 prevent formation of toxic recombination intermediates from single-stranded gaps created by DNA replication. Proc. Natl. Acad. Sci. USA **99:** 16887–16892.

Foster, P. L., 2006 Methods for determining spontaneous mutation rates. Methods Enzymol. **409:** 195–213.

Gangloff, S., C. Soustelle and F. Fabre, 2000 Homologous recombination is responsible for cell death in the absence of the Sgs1 and Srs2 helicases. Nat. Genet. **25:** 192–194.

Gerring, S. L., C. Connelly and P. Hieter, 1991 Positional mapping of genes by chromosome blotting and chromosome fragmentation. Methods Enzymol. **194:** 57–77.

Gravel, S., J. R. Chapman, C. Magill and S. P. Jackson, 2008 DNA helicases Sgs1 and BLM promote DNA double-strand break resection. Genes Dev. **22:** 2767–2772.

Irwin, B., M. Aye, P. Baldi, N. Beliakova-Bethell, H. Cheng *et al.*, 2005 Retroviruses and yeast retrotransposons use overlapping sets of host genes. Genome Res. **15:** 641–654.

Ivessa, A. S., B. A. Lenzmeier, J. B. Bessler, L. K. Goudsouzian, S. L. Schnakenberg *et al.*, 2003 The Saccharomyces cerevisiae helicase Rrm3p facilitates replication past nonhistone protein-DNA complexes. Mol. Cell **12:** 1525–1536.

Ivessa, A. S., J. Q. Zhou, V. P. Schulz, E. K. Monson and V. A. Zakian, 2002 Saccharomyces Rrm3p, a 5′ to 3′ DNA helicase that promotes replication fork progression through telomeric and subtelomeric DNA. Genes Dev. **16:** 1383–1396.

Ivessa, A. S., J. Q. Zhou and V. A. Zakian, 2000 The Saccharomyces Pif1p DNA helicase and the highly related Rrm3p have opposite effects on replication fork progression in ribosomal DNA. Cell **100:** 479–489.

Ke, N., X. Gao, J. B. Keeney, J. D. Boeke and D. F. Voytas, 1999 The yeast retrotransposon Ty5 uses the anticodon stem-loop of the initiator methionine tRNA as a primer for reverse transcription. RNA **5:** 929–938.

Kim, J. M., S. Vanguri, J. D. Boeke, A. Gabriel and D. F. Voytas, 1998 Transposable elements and genome organization: a comprehensive survey of retrotransposons revealed by the complete Saccharomyces cerevisiae genome sequence. Genome Res. **8:** 464–478.

Klein, H. L., 2001 Mutations in recombinational repair and in checkpoint control genes suppress the lethal combination of srs2Δ with other DNA repair genes in *Saccharomyces cerevisiae*. Genetics **157:** 557–565.

Krejci, L., S. Van Komen, Y. Li, J. Villemain, M. S. Reddy *et al.*, 2003 DNA helicase Srs2 disrupts the Rad51 presynaptic filament. Nature **423:** 305–309.

Lee, B. S., C. P. Lichtenstein, B. Faiola, L. A. Rinckel, W. Wysock *et al.*, 1998 Post-translational inhibition of Ty1 retrotransposition by nucleotide excision repair/transcription factor TFIIH subunits Ssl2p and Rad3p. Genetics **148:** 1743–1761.

Liu, Y.-G., and R. F. Whittier, 1995 Thermal asymmetric interlaced PCR: automatable amplification and sequencing of insert end fragments from P1 and YAC clones for chromosome walking. Genomics **25:** 674–681.

Luke, B., G. Versini, M. Jaquenoud, I. W. Zaidi, T. Kurz *et al.*, 2006 The cullin Rtt101p promotes replication fork progression through damaged DNA and natural pause sites. Curr. Biol. **16:** 786–792.

Matsuda, K., M. Makise, Y. Sueyasu, M. Takehara, T. Asano *et al.*, 2007 Yeast two-hybrid analysis of the origin recognition complex of Saccharomyces cerevisiae: interaction between subunits and identification of binding proteins. FEMS Yeast Res. **7:** 1263–1269.

Maxwell, P. H., and M. J. Curcio, 2007a Host factors that control long terminal repeat retrotransposons in Saccharomyces cerevisiae: implications for regulation of mammalian retroviruses. Eukaryot. Cell **6:** 1069–1080.

Maxwell, P. H., and M. J. Curcio, 2007b Retrosequence formation restructures the yeast genome. Genes Dev. **21:** 3308–3318.

Melamed, C., Y. Nevo and M. Kupiec, 1992 Involvement of cDNA in homologous recombination between Ty elements in Saccharomyces cerevisiae. Mol. Cell. Biol. **12:** 1613–1620.

Mimitou, E. P., and L. S. Symington, 2008 Sae2, Exo1 and Sgs1 collaborate in DNA double-strand break processing. Nature **455:** 770–774.

Mou, Z., A. E. Kenny and M. J. Curcio, 2006 Hos2 and Set3 promote integration of Ty1 retrotransposons at tRNA genes in *Saccharomyces cerevisiae*. Genetics **172:** 2157–2167.

Muller, F., W. Laufer, U. Pott and M. Ciriacy, 1991 Characterization of products of TY1-mediated reverse transcription in Saccharomyces cerevisiae. Mol. Gen. Genet. **226:** 145–153.

Ooi, S. L., D. D. Shoemaker and J. D. Boeke, 2003 DNA helicase gene interaction network defined using synthetic lethality analyzed by microarray. Nat. Genet. **35:** 277–286.

Prado, F., and A. Aguilera, 2005 Impairment of replication fork progression mediates RNA polII transcription-associated recombination. EMBO J. **24:** 1267–1276.

Schmidt, K. H., K. L. Derry and R. D. Kolodner, 2002 Saccharomyces cerevisiae RRM3, a 5′ to 3′ DNA helicase, physically interacts with proliferating cell nuclear antigen. J. Biol. Chem. **277:** 45331–45337.

Schmidt, K. H., and R. D. Kolodner, 2004 Requirement of Rrm3 helicase for repair of spontaneous DNA lesions in cells lacking Srs2 or Sgs1 helicase. Mol. Cell. Biol. **24:** 3213–3226.

Schmidt, K. H., and R. D. Kolodner, 2006 Suppression of spontaneous genome rearrangements in yeast DNA helicase mutants. Proc. Natl. Acad. Sci. USA **103:** 18196–18201.

Scholes, D. T., M. Banerjee, B. Bowen and M. J. Curcio, 2001 Multiple regulators of Ty1 transposition in *Saccharomyces cerevisiae* have conserved roles in genome maintenance. Genetics **159:** 1449–1465.

Sharon, G., T. J. Burkett and D. J. Garfinkel, 1994 Efficient homologous recombination of Ty1 element cDNA when integration is blocked. Mol. Cell. Biol. **14:** 6540–6551.

Shin, J. H., and Z. Kelman, 2006 The replicative helicases of bacteria, archaea, and eukarya can unwind RNA-DNA hybrid substrates. J. Biol. Chem. **281:** 26914–26921.

Sundararajan, A., B. S. Lee and D. J. Garfinkel, 2003 The Rad27 (Fen-1) nuclease inhibits Ty1 mobility in *Saccharomyces cerevisiae*. Genetics **163:** 55–67.

Torres, J. Z., S. L. Schnakenberg and V. A. Zakian, 2004 Saccharomyces cerevisiae Rrm3p DNA helicase promotes genome integrity by preventing replication fork stalling: viability of *rrm3* cells requires the intra-S-phase checkpoint and fork restart activities. Mol. Cell. Biol. **24:** 3198–3212.

Umezu, K., M. Hiraoka, M. Mori and H. Maki, 2002 Structural analysis of aberrant chromosomes that occur spontaneously in diploid *Saccharomyces cerevisiae*: retrotransposon Ty1 plays a crucial role in chromosomal rearrangements. Genetics **160:** 97–110.

Veaute, X., J. Jeusset, C. Soustelle, S. C. Kowalczykowski, E. Le Cam *et al.*, 2003 The Srs2 helicase prevents recombination by disrupting Rad51 nucleoprotein filaments. Nature **423:** 309–312.

Weinstock, K. G., M. F. Mastrangelo, T. J. Burkett, D. J. Garfinkel and J. N. Strathern, 1990 Multimeric arrays of the yeast retrotransposon Ty. Mol. Cell. Biol. **10:** 2882–2892.

Xu, H., and J. D. Boeke, 1991 Inhibition of Ty1 transposition by mating pheromones in Saccharomyces cerevisiae. Mol. Cell. Biol. **11:** 2736–2743.

Zhu, Z., W. H. Chung, E. Y. Shim, S. E. Lee and G. Ira, 2008 Sgs1 helicase and two nucleases Dna2 and Exo1 resect DNA double-strand break ends. Cell **134:** 981–994.

Communicating editor: D. Voytas

GENETICS

Supporting Information

http://www.genetics.org/cgi/content/full/genetics.109.104208/DC1

Rrm3 Protects the *Saccharomyces cerevisiae* Genome From Instability at Nascent Sites of Retrotransposition

Radostina Stamenova, Patrick H. Maxwell, Alison E. Kenny and M. Joan Curcio

DOI: 10.1534/genetics.109.104208

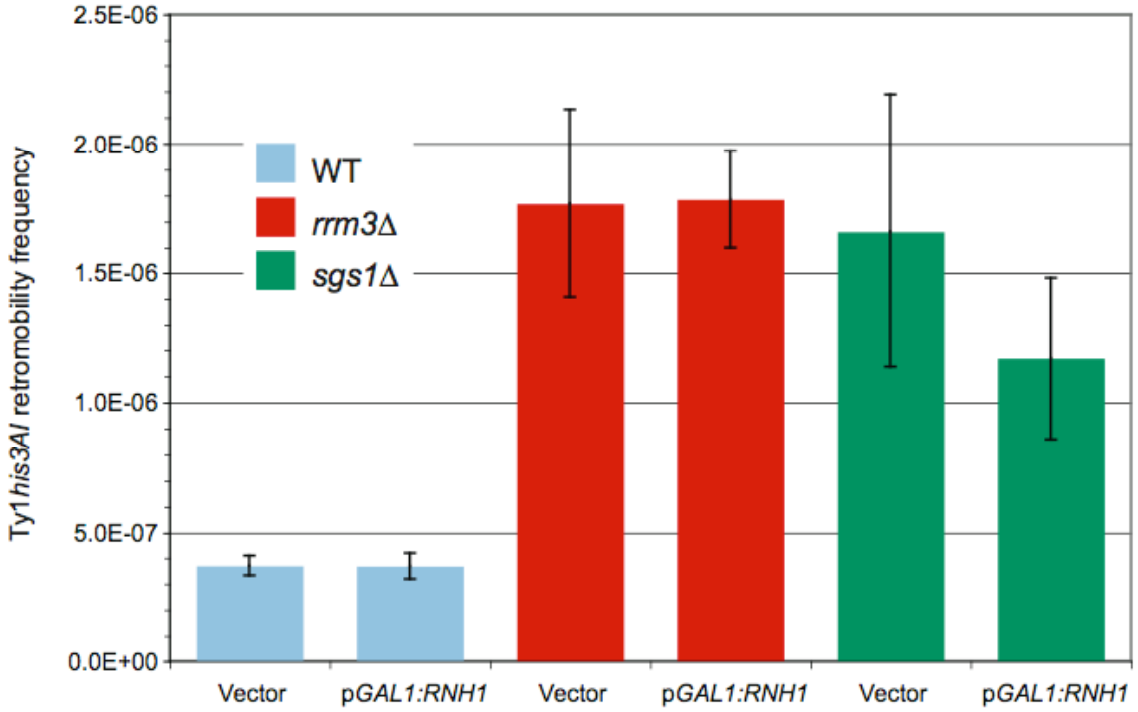

FIGURE S1.—Overexpression of RNase H does not effect the frequency of Ty1*his3AI* retromobility. Strains JC3212, JC3917 and JC4915 transformed with plasmid pRS416 or p*GAL1*:*RNH1* were grown overnight in SC-Ura glucose broth at 30°. Cells were pelleted and resuspended in an equal volume of H20. Cells were diluted 1:100 into 4 ml SC-Ura galactose broth, divided into 4 cultures and grown to saturation at 20°. An equal volume of YPD broth was added to each culture, and the cultures were incubated for 18 to 20 hr at 20˚. Aliquots of each culture were plated on SC-Ura and SC-Ura-His glucose agar. Plates were incubated for three days at 30˚ and the colonies were counted. The retromobility frequency is the average of the number of His+ Ura+ colonies divided by the total number of Ura+ colonies that retained the vector or p*GAL1*:*RNH1* plasmid throughout incubation at 20˚. The average of three experiments is presented. Error bars, standard error.

TABLE S1

Sequences flanking the 3' end of Ty1*HIS3* retromobility events

A. Ty1*HIS3* recombination events in *rrm3*Δ mutant

His+ isolate	Chromosome	Coordinate	RNA pol III-transcribed gene within 825 bp	Other features of Ty1*HIS3* junction
rrm3-26 rrm3-76 rrm3-87 rrm3-91 rrm3-105 rrm3-106 rrm3-128 rrm3-136 rrm3-139 rrm3-148	Unknown	Unknown	Unknown	At LTR-*TYA1* boundary of a Ty1 element, in the same orientation

B. Ty1*HIS3* integration events in *rrm3*Δ mutant

rrm3-1	VII	661455	*tT(UGU)G1*	298 bp upstream of *tT(UGU)G*, same orientation
rrm3-2	III	142880	*SUF16*	In *YCRCdelta7*; 111 bp upstream of *SUF16*, same orientation
rrm3-3	X	538434	*HSX1*	114 bp upstream of *HSX1*, same orientation
rrm3-4	IV	645389	*tQ(UUG)D2*	168 bp upstream of *tQ(UUG)D2*, same orientation
rrm3-5	XIII	589800	—	251 bp upstream of *MSS11* ORF; 293 bp downstream of *PAH1* ORF
rrm3-6	VII	287653	*tW(CCA)G1*	192 bp upstream of *tW(CCA)G1*, same orientation
rrm3-7	XII	489250	*RDN5-3, -5 or -6*	In *YLR156W*, *-159W* or *-161W* (identical uncharacterized ORFs); 100 bp upstream of *RDN5-3, -5* or *-6*, opposite orientation
rrm3-8	XV	594514	*SUF5*	At 5' boundary of *YORWdelta12*, opposite orientation; 88 bp upstream of *SUF5*, same orientation
rrm3-9	XVI	776388	*tC(GCA)P2*	In *YPRWdelta14*; 554 bp upstream of *tC(GCA)P2*, opposite orientation
rrm3-10	IV	645389	*tQ(UUG)D2*	168 bp upstream of *tQ(UUG)D2*, same orientation
rrm3-13	XI	379220	*tV(AAC)K2*	103 bp upstream of *tV(AAC)K2*, same

				orientation
rrm3-14	XII	468334	*RDN5-2*	480 bp upstream of *RDN5-2*, same orientation
rrm3-15	VII	779527	*SUF4*	94 bp upstream of *SUF4*, opposite orientation
rrm3-18	II	9406	*tL(UUA)B1*	In *YBLWdelta2*; 177 bp upstream of *tL(UUA)B1*, same orientation
rrm3-28	XVI	560830	*tF(GAA)P1*	544 bp upstream of *tF(GAA)P1*, opposite orientation
rrm3-35	XII	468450	*RDN5-2*	364 bp upstream of *RDN5-2*, same orientation
rrm3-38	XV	673755	—	1343 bp upstream of *SYC1* ORF; 598 bp downstream of *DCI1* ORF
rrm3-39	VII	701357	*tK(UUU)G2*	305 bp upstream of *tK(UUU)G2*, opposite orientation
rrm3-73	Unknown	Unknown	Unknown	At +105 of Ty2 LTR, opposite orientation
rrm3-88	VII	701279	*tK(UUU)G2*	In *YGRWdelta19*; 227 bp upstream of *tK(UUU)G2*, opposite orientation
rrm3-96	XVI	859967	*tG(GCC)P2*	408 bp upstream of *tG(GCC)P2*, same orientation
rrm3-97	Unknown	Unknown	Unknown	At +289 of Ty4 LTR, opposite orientation
rrm3-98	Unknown	Unknown	Unknown	At +177 of Ty1 LTR, opposite orientation
rrm3-99	X	234028	*tR(ACG)J*	21 bp downstream of *tR(ACG)J*
rrm3-101	II	401157	—	273 bp upstream of *SEC18* ORF; 90 bp downstream of *SPT7* ORF
rrm3-102	VII	931850	*tG(GCC)G2*	In *YGRWdelta32*; 824 bp upstream of *tG(GCC)G2*, same orientation
rrm3-120	VII	701235	*tK(UUU)G2*	In *YGRWdelta19*; 183 bp upstream of *tK(UUU)G2*, same orientation
rrm3-127	XIV	102518	*tN(GUU)N1*	In 5' LTR of *YNLCTy1-1*; 198 bp upstream of *tN(GUU)N1*, same orientation
rrm3-129	XI	302193	*tW(CCA)K*	In *YKLCdelta5*; 369 bp upstream of *tW(CCA)K*, same orientation
rrm3-130	XIV	570064	*tI(AAU)N1*	123 bp upstream of *tI(AAU)N1*, same orientation
rrm3-146	XVI	810499	*tN(GUU)P*	In 5' LTR of *YPRCTy1-2*; 173 bp upstream of *tN(GUU)P*, same orientation

C. Ty1*HIS3* integration events in wild-type strain

wt-23	X	374758	*tR(UCU)J2*	186 bp upstream of *tR(UCU)J2*, opposite orientation

wt-27	II	644957	*tE(UUC)B*	205 bp upstream of *tE(UUC)B*, opposite orientation
wt-29	XI	302481	*tW(CCA)K*	81 bp upstream of *tW(CCA)K*, opposite orientation
wt-30	Unknown	Unknown	Unknown	At +346 of Ty4 LTR, same orientation
wt-31	Unknown	Unknown	Unknown	At +150 of Ty1 LTR, same orientation
wt-33	VII	74252	*tV(AAC)G3*	351 bp upstream of *tV(AAC)G3*, opposite orientation
wt-34	XII	489250	*RDN5-3, -5* or *-6*	In *YLR156W*, *-159W* or *-161W*; 100 bp upstream of *RDN5-3, -5 or -6*, opposite orientation
wt-36	IV	803215	*tQ(UUG)D3*	In *YDRWdelta11*; 416 bp upstream of *tQ(UUG)D3*, opposite orientation
wt-37	XI	74360	*tN(GUU)K*	In *YKLWdelta1*; 269 bp upstream of *tN(GUU)K*, same orientation
wt-38	V	441821	*SCR1*	In *YER137C*, uncharacterized ORF; 162 bp upstream of *SCR1*, opposite orientation
wt-42	Unknown	Unknown	Unknown	At +169 of Ty4 LTR, opposite orientation
wt-44	V	138480	*tR(UCU)E*	In *YELWdelta6*; 186 bp upstream of *tR(UCU)E*, same orientation
wt-46	IV	1151138	*tX(XXX)D*	In *YDRWdelta25*; in *YDR340W*, dubious ORF; 203 bp upstream of *tX(XXX)D*, same orientation
wt-54	II	750025	—	At +436 in *CHK1* ORF, same orientation
wt-56	XIII	168360	*SUP5*	435 bp upstream of *SUP5*, opposite orientation